Pol. J. Environ. Stud. Vol. XX, No. X (XXXX), 1-14
DOI: *10.15244/pjoes/225153* ONLINE PUBLICATION DATE: 31-08-2026

Original Research

Effects of Microplastic Type and Ageing on Cadmium Adsorption

Qihang Li[1, 2], Anna Bogush[3], Pan Wu[1, 2]*

[1]Key Laboratory of Karst Georesources and Environment (Guizhou University), Ministry of Education, Guiyang, China
[2]College of Resources and Environmental Engineering, Guizhou University, Guiyang, China
[3]Centre for Agroecology, Water and Resilience, Coventry University, Coventry, UK

Received: 25 February 2026
Accepted: 27 June 2026

Abstract

Microplastics (MPs) can adsorb cadmium (Cd) and influence its environmental fate. However, the roles of polymer type and ageing in governing Cd adsorption remain insufficiently understood. This study systematically investigated Cd adsorption onto virgin and H_2O_2-aged polyethylene (PE), polyvinyl chloride (PVC), and polylactic acid (PLA) under controlled aqueous conditions. Adsorption experiments, coupled with isotherm and kinetic modelling and supported by surface characterisation (SEM–EDS, FTIR, and zeta-potential analyses), revealed that Cd adsorption is better described by the Langmuir model, indicating site-limited adsorption with saturation, and follows pseudo-second-order kinetics. Polymer type was the dominant control on Cd uptake (PLA>PVC>PE), irrespective of ageing state. PLA exhibited the highest maximum adsorption capacity (Q_{max}) and strongest affinity, consistent with its higher abundance of oxygen-containing functional groups, more negative surface charge, and greater surface roughness. Ageing effects were polymer-specific: ageing markedly enhanced adsorption affinity and low-concentration sensitivity for PLA, produced a more moderate enhancement for PVC, and had minimal influence on PE. These findings demonstrate that polymer chemistry fundamentally governs baseline Cd adsorption, while ageing modulates adsorption affinity in a polymer-dependent manner. This study provides new mechanistic insight into how biodegradable and conventional MPs differentially interact with toxic metals, improving our understanding of metal partitioning at the water–MPs interface and informing risk assessments of MP-associated metal transport in aquatic environments.

Keywords: microplastics, Cd, adsorption, MP type, PLA

Introduction

Microplastics (MPs), defined as plastic particles smaller than 5 mm [1], are now ubiquitous across aquatic and terrestrial ecosystems [2]. They originate from various sources, including the breakdown of larger plastic debris, industrial processes, agricultural practices, and the use of personal care products [3-5]. In addition to these sources, human-driven activities such as tourism, recreation, urbanisation, and agricultural production can influence the occurrence and spatial distribution of MPs in the environment [6]. Once

*e-mail: pwu@gzu.edu.cn
Tel: +86-13885030478
0000-0003-1083-3025

released, MPs can persist for decades owing to their resistance to natural degradation [7]. Their extensive presence in the environment has raised significant concern because MPs negatively affect aquatic and terrestrial ecosystems [8]. For example, MPs can suffocate and smother benthic marine organisms, affect soil structure, harm soil microbiota, and deplete soil nutrients [9-11]. These alterations affect ecological functions, plant growth, microbial activity, and overall ecosystem stability [12].

Cadmium (Cd) is a highly toxic heavy metal that poses significant risks to ecosystems and human health [13]. Cd can persist in the environment for centuries [14]. It mainly originates from natural processes, such as the weathering of parent rocks, and human activities, including industrial emissions, mining, smelting, and the use of phosphate fertilisers and sewage sludge [15, 16]. Cd readily accumulates in soil and sediments, where it disrupts microbial communities, reduces biodiversity, and impairs ecological functions, ultimately constraining plant growth [17]. More importantly, Cd can enter the food chain through crop uptake, ultimately posing serious health risks to humans [18].

Recent studies show that MPs and Cd interact in ways that can modify Cd mobility, partitioning, and ecological effects in the environment [19-22]. MPs can act as transport vectors of heavy metals, concentrating them on their particle surfaces and potentially facilitating redistribution through their movement [23]. Adsorption of Cd onto MPs is controlled largely by the surface properties of MP particles, such as charge, functional groups, roughness, and the presence of additives or weathering-derived oxidation products, which together determine the availability of binding sites and the strength of Cd association [24]. Additionally, MPs affect the fate of heavy metals by altering soil physicochemical properties, which regulate Cd speciation and bioavailability. For example, Erdem et al. [25] and Huang et al. [20] found that MPs decreased soil pH, thereby increasing Cd solubility and bioavailability, and polyethylene (PE) had a greater effect than PS [20]. MPs have also been shown to modify Cd partitioning among soil fractions; for example, PP MPs promoted Cd transfer from organo-mineral complexes to particulate organic matter, increasing the available Cd concentration; this effect depends on MPs' properties, such as size and concentration [26]. Furthermore, the combined impact of MPs and Cd on environmental health varies across different studies. Huang et al. [27] indicated that co-exposure to pollutants can lead to synergistic toxicity, resulting in greater harm than each pollutant alone. Conversely, Liu et al. [28] suggested that MPs can reduce Cd toxicity under certain conditions.

The Cd adsorption capacity of MPs varies with MP size, polymer type, shape, ageing, and concentration [21, 29]. Smaller MP particles generally have a higher adsorption capacity due to their larger surface area [29]. Polymer chemistry also plays an important role: polyvinyl chloride (PVC) often shows higher Cd sorption than PE and PP, indicating differences in surface polarity and potential binding interactions [30]. Ageing processes, including oxidative weathering, can further alter MPs' surfaces by increasing roughness and introducing oxygen-containing functional groups that may enhance metal binding [31]. Despite these advances, the relative roles of polymer type and ageing in influencing Cd adsorption by MPs remain insufficiently resolved. Previous studies have focused on individual polymers, specific ageing conditions, or MP size [32, 33], making it difficult to directly compare the effects of polymer chemistry with those of surface changes after ageing. Direct comparisons between conventional plastics and biodegradable alternatives under the same experimental conditions are also limited [34, 35]. These gaps limit mechanistic understanding and constrain our ability to predict how emerging biodegradable MPs may influence metal behaviour relative to conventional plastics.

The main goal of this research is to investigate the influence of microplastic type and ageing processes on Cd adsorption. In this study, three MP types were selected to represent contrasting polymer chemistries: PE, a common polyolefin with a relatively inert hydrophobic surface; PVC, a chlorine-containing conventional plastic with different surface polarity and elemental composition; and PLA, a representative biodegradable biobased polyester containing oxygen-bearing functional groups [33, 38]. This selection allows comparison among polymers with distinct surface properties and between conventional plastics and a biodegradable biobased alternative under the same experimental conditions. Other common polymers, such as PS and PP, are frequently reported in the literature [29]. However, they were not included as the present study focused on these three chemically contrasting polymers and on the comparison between virgin and oxidatively aged states.

Materials and Methods

Microplastics

PE, PVC, and PLA MPs were obtained from a commercial supplier (Taobao). PE and PVC are widely used in agricultural applications [36, 37], while PLA is a biodegradable and biobased polymer increasingly proposed as an alternative mulching material [38]. The MPs were in fragment form. All samples were dry-sieved through 100-200 mesh sieves to obtain the 75-150 μm size fraction. This morphology and size fraction were selected because fragments represent a dominant form of environmental MPs, and small MPs (<150 μm) account for a substantial proportion of environmental MP inventories [39, 40]. Ageing was conducted by immersing MPs in 30% hydrogen peroxide (H_2O_2) at 35ºC for 7 days [41, 42]. The aged MPs were then dried at 35ºC for 3 days. Polymer identity was

verified using Fourier transform infrared spectroscopy (FTIR; IRTracer-100, Shimadzu, Japan), and MPs' surface morphology was examined by scanning electron microscopy (SEM; SIGMA 300, Zeiss, Germany). The zeta potential of MPs was measured using electrophoretic light scattering (ELS; Malvern Panalytical-Zetasizer Pro, UK) at pH 6.0 (±0.1), low salinity (deionised water, I ≈ 0), and room temperature (25±0.5ºC). Dried MPs were dispersed in the specified medium to form a dilute suspension to prevent multiple scattering at high concentrations. Before zeta-potential measurement, the suspensions were sonicated for 2-5 min until visually uniform dispersion was achieved. The same dispersion-based criterion was applied to all materials and replicates, and the sonication time was not treated as an experimental variable. Sonication was kept short to minimise the potential fragmentation of MP particles caused by excessive sonication. Three suspension samples were prepared for each material, with each measured at least three times. Results are expressed as mean±standard deviation (SD) (Table 1). Conductivity and count rate were also recorded for quality control.

Adsorption Experiment

Isothermal Adsorption

A Cd solution (100 mg/L as Cd^{2+}) was prepared by dissolving analytical-grade cadmium chloride ($CdCl_2$) in distilled water. Working solutions were prepared by serial dilution to 0.5, 1, 2, 5, 10, 20, 50, and 100 mg/L. The pH was adjusted to 6.0±0.1 with dilute HNO_3/NaOH.

For the adsorption experiment, 100 mL of the Cd solution was placed in a glass bottle, and approximately 0.1 g of MPs (PE, PVC, or PLA) was added, equivalent to 1 g/L. Bottles were shaken in a thermostatic water-bath shaker (25ºC, 48 h). The suspension samples were then filtered through a 0.45 µm membrane, and the Cd concentration was analysed in the filtrates by Inductively Coupled Plasma-Optical Emission Spectrometry (ICP-OES, iCAP 7200 Thermo Scientific). The retained MPs were collected and dried for post-adsorption characterisation (e.g., SEM). All experiments were run in triplicate. Scanning electron microscopy with energy-dispersive X-ray spectroscopy (SEM-EDS) was used to investigate the Cd distribution on the surface of MPs.

The Cd adsorption capacity of MPs (Q_e, mg/g) was determined using the following Equation:

$$Q_e = \frac{(C_0 - C_e)V}{m}$$

Where C_0 is the measured Cd concentration in the procedural blank without MPs for each nominal concentration, C_e is the equilibrium Cd concentration in the MP treatment (mg/L), V is the volume of the Cd solution (L), and m is the mass of the MPs (g).

Cd removal efficiency (RE, %) for each investigated MP type was calculated using the following Equation:

$$RE = \frac{C_0 - C_t}{C_0} \times 100$$

The results from the adsorption experiments were interpreted according to the Langmuir and Freundlich adsorption isotherms. The Langmuir and Freundlich isotherms [43] were fitted using non-linear least squares, as they offer complementary descriptions of equilibrium behaviour (capacity/affinity versus heterogeneity/low–mid concentration performance), as detailed below.

Langmuir Isotherm Model

$$Qe = \frac{Q_{max} K_L C_e}{1 + K_L C_e}$$

Where Q_{max} (mg/g) is the monolayer capacity and K_L (L/mg) is the affinity constant. Useful derived quantities include initial slope $S_0 = Q_{max}\ K_L$ (L/g) and half-saturation concentration $C_{50} = 1/K_L$ (mg/L).

Freundlich Isotherm Model

$$Qe = K_F C_e^{1/n}$$

Table 1. Zeta potential of MPs, mV.

Number	Re1	Re2	Re3	Mean	SD
PE-N	-10.90	-11.20	-11.97	-11.36	0.45
PE-A	-13.02	-11.81	-13.76	-12.86	0.80
PVC-N	-22.50	-21.28	-22.10	-21.96	0.51
PVC-A	-24.81	-24.23	-23.64	-24.23	0.48
PLA-N	-32.15	-31.89	-32.26	-32.10	0.16
PLA-A	-37.28	-38.12	-39.06	-38.15	0.73

Note: "N" denotes "virgin MPs"; "A" denotes "aged MPs".

Where K_F reflects capacity (units $mg^{1-1/n}\ g^{-1}\ L^{1/n}$), and n>1 indicates favourable adsorption on heterogeneous surfaces.

Kinetic Experiments

Kinetic experiments also provide important information on the adsorption mechanism. These experiments were performed at a Cd concentration of 5 mg/L, a mid-range concentration often used in MP-metal batch studies [44], with the same liquid volume, dose, and temperature as the adsorption isotherm experiments, with sampling times of 5, 10, 30, 60, 120, 240, 360, 480, 720, 960, 1440, and 2880 min. The experiment was run in triplicate. The collected suspensions were filtered through a 0.45 μm membrane, and dissolved Cd in the filtrate was measured by ICP–OES. To quantify the approach to equilibrium without assuming a specific mechanism, pseudo-first-order (PFO) and pseudo-second-order (PSO) models [45] were fitted using nonlinear least squares, yielding equilibrium uptake, rate constants, and interpretable timescales ($t_{1/2}$, t_{90}).

$$Q_t = \frac{(C_0 - C_t)V}{m}$$

Where Q_t (mg/g) indicates the uptake at time t (min), and C_t is the Cd concentration at time t (mg/L).

Pseudo-First-Order Model

$$Q_t = Q_e(1 - e^{-k1t})$$

Where Q_e (mg/g) represents the fitted equilibrium uptake under kinetic conditions, and k1 (min^{-1}) denotes the PFO rate constant. Half-time: $t_{1/2} = \ln 2/k_1$; $t_{90} = 2.303/k_1$.

Pseudo-Second-Order Model

$$Q_t = \frac{K_2 Q_e^2 t}{1 + K_2 Q_e t}$$

Where k_2 (g/mg/ min) represents the PSO rate constant. Half-time: $t_{1/2} = 1/(k_2 Q_e)$; $t_{90} = 9/(k_2 Q_e)$. The initial rate, $h = k_2 Q_e^2$ (mg/g/min), is also provided.

Quality Control

A procedural blank without MPs (CK) was processed alongside all tests and analysed in the same way as the samples. Concentrations used in mass-balance calculations were blank-corrected where applicable. Solution pH was verified at the start and end of each batch experiment (6.0±0.1). All glassware and filtration systems used were pre-cleaned and thoroughly rinsed with deionised water. The ICP-OES was calibrated using multi-point Cd standards (traceable) and checked with ongoing calibration verification; recalibration was initiated if the continuing calibration verification (CCV) deviated by more than 10%. For each condition and time point, the experiments were run in triplicate, and the results were reported as mean ± SD.

Statistical Analysis

Statistical analyses were performed using IBM SPSS Statistics (Version 26.0, IBM Corp., Armonk, NY, USA). Data are presented as mean±standard deviation (SD) from three independent experimental bottles (n = 3). For each MP type and ageing condition, differences among initial Cd concentrations were assessed by one-way analysis of variance (ANOVA), followed by Fisher's least significant difference (LSD) post-hoc test. Statistical significance was accepted at $p<0.05$. Nonlinear regressions for isotherm and kinetic models were performed in Microsoft Excel using the Solver add-in (GRG Nonlinear) with least-squares minimisation, and figures were generated in Excel.

Results

Surface Characteristics of Mps

All aged MPs exhibit pronounced surface roughening and fissuring (Fig. 1). Virgin PE presents a relatively smooth surface with shallow craze lines; following ageing, PE develops mild granular roughness accompanied by shallow grooves. Virgin PVC is characterised by nodular or granular surface protrusions, which, upon ageing, coalesce into an extensive porous network with enlarged pits and interparticle voids. PLA displays distinct ridged or lamellar surface features; ageing induces pronounced lamellar exfoliation, deeper surface cracking, and increased microporosity. These observations indicate that PLA undergoes more substantial topographical alteration during ageing compared with PE and PVC.

The FTIR spectra of the three polymers are shown in Fig. 2. PLA displayed a distinct ester carbonyl band at ~1750-1760 cm^{-1} and strong C–O/C–O–C stretching bands in the 1050-1250 cm^{-1} region. After ageing, a broad band developed at ~3200-3600 cm^{-1}, and the bands at ~1750-1760 cm^{-1} and 1050-1250 cm^{-1} increased in intensity and became broader. PVC exhibited C–H stretching bands at 2850-2960 cm^{-1}, a CH_2 deformation band near ~1425 cm^{-1}, and a pronounced absorption region at ~600-700 cm^{-1}. Compared with virgin PVC, the aged PVC spectrum showed higher intensity and broader features across the fingerprint region (1500-600 cm^{-1}). A subtle increase was also observed around ~1000–1100 cm^{-1}. PE was characterised by CH_2 stretching bands at 2915/2848 cm^{-1}, CH_2 scissoring at ~1470 cm^{-1}, and CH_2 rocking at ~720 cm^{-1}. No distinct

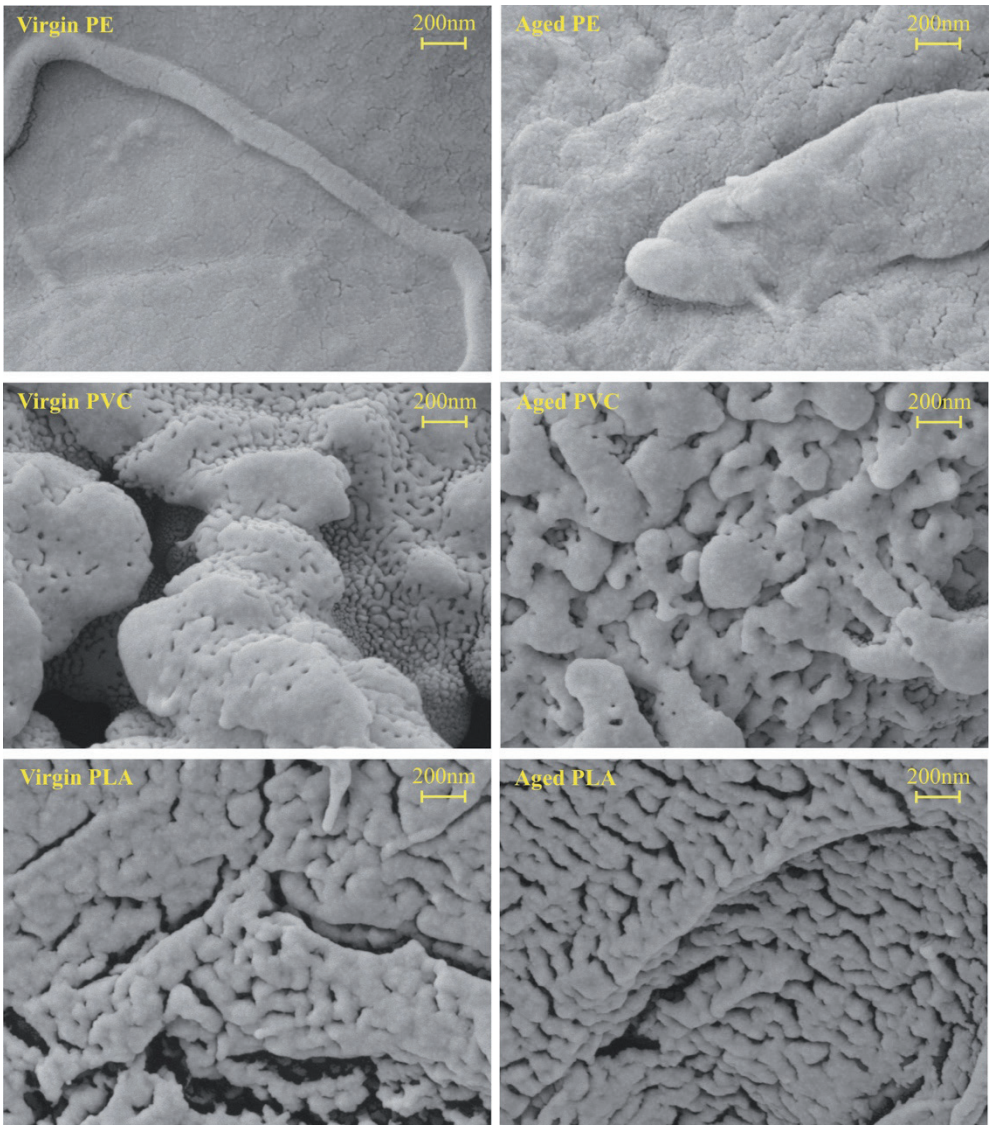

Fig. 1. Surface morphology analysis of MPs using SEM.

carbonyl (~1700-1800 cm^{-1}) or O–H (~3200-3600 cm^{-1}) bands were observed for PE, and ageing led to only minor changes in band shape and intensity.

Cd Removal by MPs

The extent of removal and adsorption capacity depends on the initial Cd concentration. In this study, we analysed the effect of eight initial Cd concentrations (0.5, 1, 2, 5, 10, 20, 50, 100 mg/L) on Cd adsorption. Fig. 3 shows the influence of initial Cd concentration on the extent of Cd removal. Overall, Cd removal efficiency remained low across all treatments and tended to decrease at higher initial Cd concentrations, although some fluctuations were observed at low to intermediate concentrations. At 0.5 mg/L, Cd removal efficiencies were 2.18%, 3.68%, 5.23%, 2.77%, 3.02%, and 7.70% for PE-N, PVC-N, PLA-N, PE-A, PVC-A, and PLA-A, respectively. At 100 mg/L, the corresponding values decreased to 0.77%, 1.15%, 1.50%, 0.79%, 1.23%, and 1.66%, respectively. Across most concentrations, PLA showed higher Cd removal than PVC and PE, while PE showed the lowest removal. Ageing generally increased Cd removal for PLA and PVC, whereas its effect on PE was limited. These results indicate that MPs had low overall Cd removal efficiency, but clear polymer-dependent differences were still observed.

Adsorption Isotherms

The Cd adsorption capacity of all MPs increased with increasing Cd concentration and then approached plateaus (Fig. 4a) and b)). The R^2 values for the Langmuir model were 0.983, 0.987, 0.985, 0.984, 0.981, and 0.983 for PE-N, PVC-N, PLA-N, PE-A, PVC-A, and PLA-A, respectively, whereas those for the Freundlich model were 0.932, 0.957, 0.948, 0.935, 0.931, and 0.931. The experimental results of Cd adsorption on MPs were well fitted by both the Langmuir and Freundlich isotherm models (R^2>0.9; Table 2). However, the Langmuir

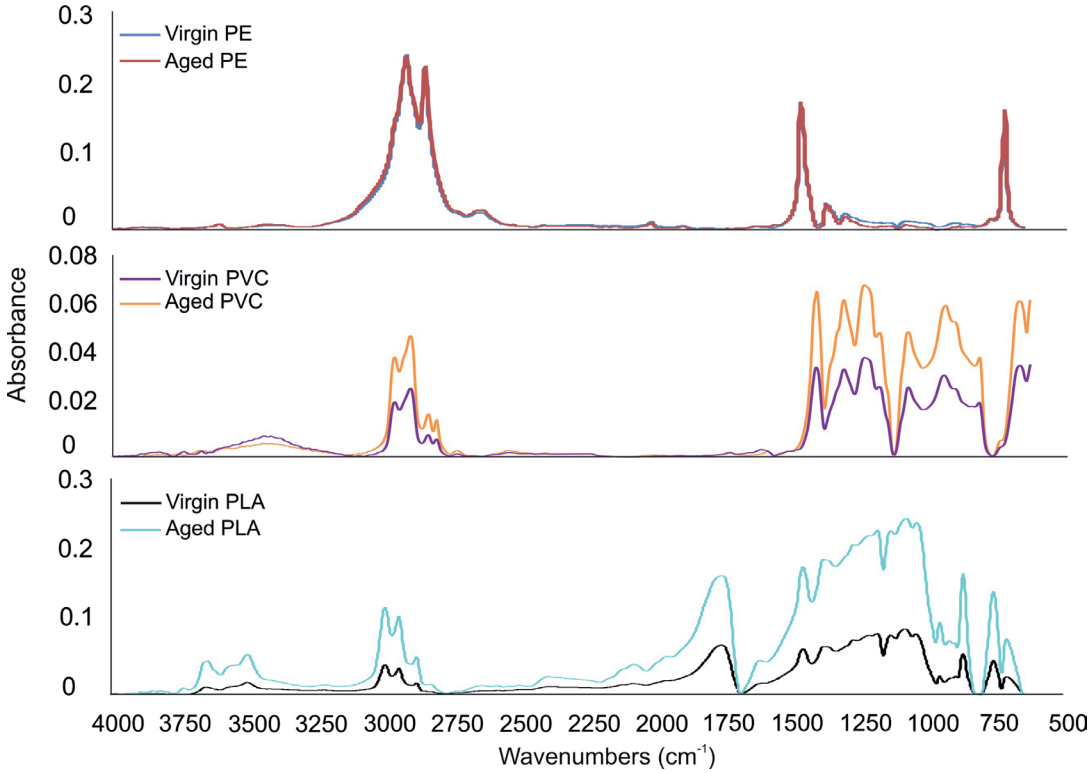

Fig. 2. FTIR spectra of virgin and aged PLA, PVC, and PE microplastics.

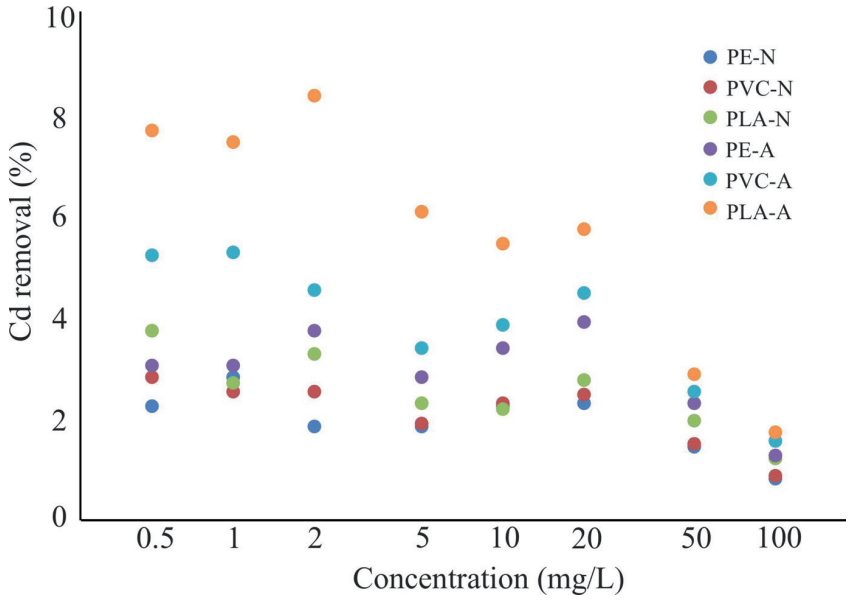

Fig. 3. The Cd removal rates of different types of MPs under various Cd concentrations.

isotherm model consistently yielded higher R^2 values than the Freundlich model for PE, PVC, and PLA (both virgin and aged).

Langmuir fits replicate the curvature and plateau at high C_e, whereas Freundlich fits capture the rise at low C_e but tend to overestimate the upper end because they lack an explicit saturation term (Fig. 4a)). In addition, ageing shifted the curves upwards, most noticeably at low to medium Cd concentrations of 10-50 mg/L. The fitted Langmuir isotherm capacities (Q_{max}) were 1.93/1.87 mg/g for PLA (virgin/aged), 1.69/1.60 mg/g for PVC, and 0.98/1.03 mg/g for PE, indicating that ageing had only a modest effect on Q_{max}, and that Cd adsorption capacity among polymer types followed the order PLA > PVC > PE. In contrast, the Langmuir affinity constant (K_L) showed clearer ageing effects for PLA and PVC, increasing from 0.031 to 0.052 and from 0.021 to 0.033 L/mg, respectively, while remaining

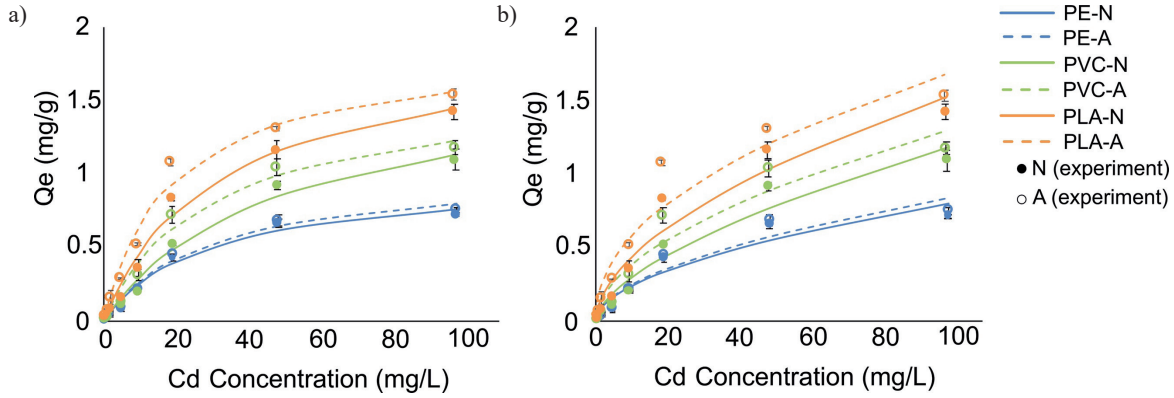

Fig. 4. Langmuir and Freundlich isotherm fits for Cd adsorption on pristine (N) and H_2O_2-aged (A) PE, PVC and PLA microplastics. a) Langmuir model and b) Freundlich model. Symbols represent experimental data, and lines represent model fits. Error bars indicate the standard deviation (SD) of three independent replicates (n = 3).

essentially unchanged for PE (Table 2). Accordingly, ageing decreased the half-saturation concentration (C_{50}) of PLA and PVC, whereas C_{50} remained nearly constant for PE. Overall, these results indicate that polymer type primarily controls the magnitude of Cd uptake, including both adsorption capacity and baseline affinity. PLA exhibits the highest uptake and, upon ageing, the strongest binding. In contrast, ageing predominantly enhances adsorption affinity, leading to an earlier approach to saturation for PLA and PVC, whereas PE remains comparatively insensitive to ageing. Consistent with this affinity enhancement, the initial adsorption coefficient (S_0) increases markedly with ageing for PLA and PVC but shows only minor changes for PE. This pattern indicates a stronger ageing effect on adsorption sensitivity at low Cd concentrations (C_e<10 mg L^{-1}) for PLA and PVC.

Adsorption Kinetics

As shown in Fig. 5a) and b), all MPs exhibited rapid Cd uptake during the initial stage (within the first 60-120 min), followed by a slower adsorption stage, and equilibrium was gradually reached after approximately 1440 min. The experimental equilibrium adsorption capacity (*qe_exp*) was calculated as the average of Q_t at the final two sampling times (Table 3). Across polymer types, *qe_exp* was higher for PLA than for PVC and PE, with values of 0.155 mg/g (PLA-N) and 0.248 mg/g (PLA-A), compared with 0.111/0.125 mg/g for PVC (PVC-N/PVC-A) and 0.081/0.085 mg/g for PE (PE-N/PE-A) (Table 3).

The kinetic experimental data were fitted using PFO and PSO models. For all MPs, PSO R^2 values ranged from 0.866 to 0.979, whereas PFO R^2 values ranged from 0.814 to 0.951 (Table 3). PSO provided higher R^2 values than PFO and yielded *qe_cal* values closer to *qe_exp* (Table 3). Based on PSO fits, ageing slightly increased *h* for PE (from 0.0443 to 0.0451 mg/g/min) and PVC (from 0.0422 to 0.0426 mg/g/min). In contrast, aged PLA showed a higher *qe_exp* but a lower *h* than virgin PLA (from 0.0689 to 0.0166 mg/g/min) (Table 3). Overall, Cd adsorption exhibited clear polymer-dependent kinetics, with faster uptake on PLA than on PVC and PE (Fig. 5a); Table 3). Ageing increased the initial adsorption rate (*h*) for PE and PVC, whereas aged PLA showed higher equilibrium uptake but a lower initial adsorption rate than pristine PLA (Table 3).

Table 2. Fitting parameters of Langmuir and Freundlich isotherm models of Cd(II) adsorption on virgin and aged PLA, PVC, and PE MPs.

Polymer	Q_{max} (mg/g)	Langmuir				Freundlich		
		K_L (L/mg)	C_{50} (mg/L)	S_0 (L/g)	R^2 (-)	K_F (mg/g)(L/mg)$^{1/n}$	*1/n* (-)	R^2 (-)
PE-N	0.984	0.034	29.51	0.033	0.983	0.069	0.535	0.932
PE-A	1.033	0.034	29.64	0.035	0.984	0.072	0.534	0.935
PVC-N	1.686	0.021	47.67	0.035	0.987	0.071	0.612	0.957
PVC-A	1.603	0.033	29.91	0.053	0.981	0.110	0.54	0.931
PLA-N	1.926	0.031	32.18	0.060	0.985	0.123	0.55	0.948
PLA-A	1.868	0.052	19.28	0.097	0.983	0.198	0.467	0.931

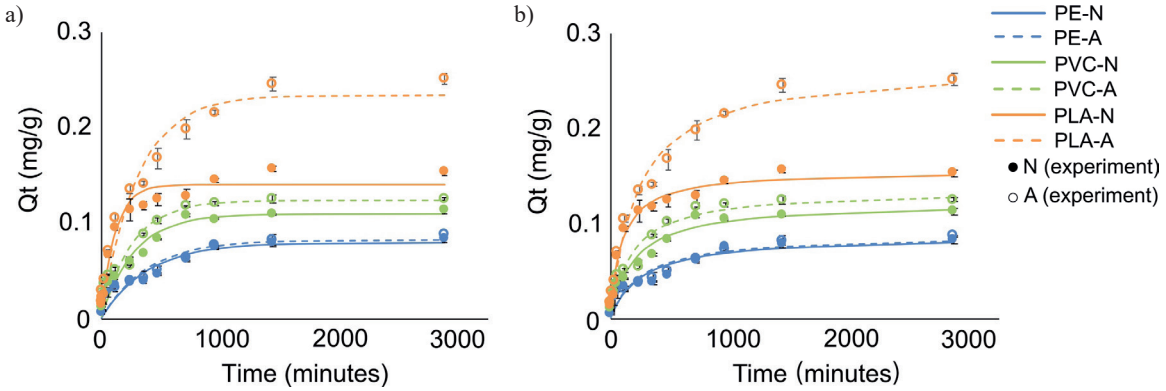

Fig. 5. Pseudo-first-order (PFO) and pseudo-second-order (PSO) kinetic model fits for Cd adsorption on pristine (N) and H_2O_2-aged (A) PE, PVC and PLA microplastics. a) PFO model and b) PSO model. Symbols represent experimental data and lines represent model fits. Error bars indicate the standard deviation (SD) of three independent replicates (n = 3).

Table 3. Fitting parameters of PFO and PSO models for Cd(II) adsorption on virgin and aged PLA, PVC, and PE MPs.

Polymer	*qe_exp*	PFO			PSO			
		qe_cal	*K1*	R^2	*qe_cal*	*K2*	R^2	*h*
	(mg/g)	(mg/g)	(1/min)	(-)	(mg/g)	(g/mg/min)	(-)	(mg/g/min)
PE-N	0.081	0.08	0.0026	0.845	0.088	0.0443	0.885	3.42×10^{-4}
PE-A	0.085	0.082	0.0026	0.814	0.09	0.0451	0.866	3.63×10^{-4}
PVC-N	0.111	0.109	0.0036	0.925	0.122	0.0422	0.946	6.30×10^{-4}
PVC-A	0.125	0.123	0.0039	0.882	0.136	0.0426	0.906	7.89×10^{-4}
PLA-N	0.155	0.139	0.0086	0.951	0.156	0.0689	0.979	1.68×10^{-3}
PLA-A	0.248	0.234	0.0033	0.944	0.266	0.0166	0.975	1.18×10^{-3}

Note: *qe_exp* = experimental equilibrium adsorption capacity; *qe_cal* = calculated equilibrium adsorption capacity; $h = K2 \cdot qe\_cal^2$

SEM-EDS Analysis

To examine the distribution of Cd on MP surfaces, SEM-EDS elemental mapping was carried out on MPs collected after the adsorption experiment at an initial Cd concentration of 100 mg/L (Fig. 6). This higher concentration was used to increase surface Cd loading and improve detectability by EDS analysis. Clear polymer-dependent differences were observed. Cd signals were readily detected on PLA (both pristine and aged) over relatively large surface areas, suggesting broadly distributed surface association. Aged PLA showed stronger Cd signals, consistent with its higher Cd uptake quantified from solution measurements. By contrast, Cd on PE appeared highly localised. On pristine PE (PE-N), Cd was observed only in isolated hotspots rather than as a continuous surface coverage. For aged PE (PE-A), no Cd signal was detected in the mapped areas despite repeated scans across multiple fields of view. Cd was also not detected on PVC under the present SEM–EDS mapping conditions. Given the low overall uptake of PE and the hotspot-like distribution observed on PE-N, the lack of detectable Cd on PE-A and PVC likely reflects low and heterogeneous surface loading close to the EDS detection limit, rather than a complete absence of adsorbed Cd.

Overall, SEM-EDS mapping provides qualitative support for Cd association with MPs and reveals marked differences in the spatial distribution of Cd across polymers. These surface observations align with the kinetic and equilibrium trends observed in solution-phase analyses, and SEM-EDS is used here as a complementary visualisation tool rather than a quantitative measure of adsorption.

Discussion

Effect of MP Type on Cd Adsorption Capacity

The results indicate that polymer type is a primary driver of differences in Cd adsorption among the investigated MPs. Across solution-phase measurements, PLA consistently exhibited higher Cd uptake than PVC and PE, as evidenced by greater removal, higher adsorption capacity, and faster uptake behaviour

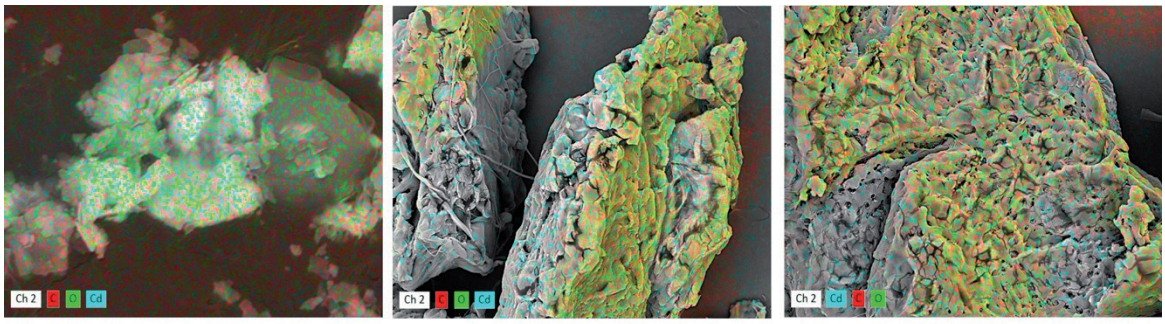

Fig. 6. Cd elemental mapping on the surface of MPs after adsorption (SEM-EDS).

(Figs. 3-5; Tables 2-3). This pattern aligns with the broad consensus that heavy metal adsorption by MPs is strongly polymer-dependent [46, 47]. Importantly, virgin and aged MPs were analysed in parallel under identical conditions in this study. The polymer-type ranking remained invariant across ageing states (PLA > PVC > PE), indicating that polymer chemistry fundamentally governs baseline adsorption behaviour, while ageing primarily modulates its magnitude rather than altering the relative hierarchy.

Isotherm analysis indicated that both virgin and aged MPs were better described by the Langmuir isotherm model, suggesting site-limited adsorption with apparent saturation at higher concentrations [48]. This behaviour is consistent with progressive occupation of a finite number of accessible surface binding sites, rather than unrestricted multilayer accumulation [49]. The Langmuir fit was therefore interpreted as being consistent with apparent monolayer adsorption under the tested conditions, while recognising that MP surfaces are heterogeneous and that electrostatic attraction, surface complexation, and roughness-related retention may jointly contribute to Cd uptake. Within each ageing state, the maximum adsorption capacity (Q_{max}) followed the order PLA > PVC > PE (Table 2), indicating stable polymer-dependent differences in saturable adsorption capacity. In general, Q_{max} reflects the number of saturable adsorption sites, whereas affinity-related parameters (K_L or C_{50}) and the initial sorption coefficient (S_0) capture adsorption strength and sensitivity at low concentrations [50]. In this study, PLA exhibited higher Q_{max} and more favourable affinity-related parameters than PVC and PE, consistent with stronger Cd uptake under the same L-type adsorption isotherm. The kinetic data aligned with the adsorption isotherm ranking. PLA showed higher *qe_exp* than PVC and PE (Table 3), and its uptake curves approached equilibrium more rapidly (Fig. 5). The better fit of the PSO model suggests that Cd uptake was closely related to surface adsorption sites and interactions between Cd ions and reactive groups on MP surfaces. This pattern may involve chemisorption-related processes [44], such as surface complexation or coordination with oxygen-containing functional groups. However, the PSO model alone does not confirm a purely chemical adsorption mechanism. The FTIR results showed ester-related C=O and C–O/C–O–C groups on PLA and stronger oxygen-related features after ageing, particularly for PLA, while the zeta potential results showed more negative surface charges for PLA than for PVC and PE. These surface characteristics suggest that Cd adsorption was likely controlled by both surface complexation and electrostatic attraction.

SEM-EDS mapping further suggested that Cd association on PE was highly heterogeneous, appearing as sparse, localised hotspots rather than broadly distributed signals. In contrast, PLA showed more spatially extensive Cd signals, consistent with its higher uptake quantified from solution-phase measurements (Fig. 6). Although the tested MPs adsorbed Cd, their removal efficiencies were relatively low compared with many natural or engineered adsorbents used for heavy metal immobilisation [44]. Natural organic materials and engineered amendments, such as humic substances, biochar, nano humic acid, and modified mineral-based adsorbents, commonly contain abundant reactive functional groups or ion-exchange sites that can provide stronger metal binding [51, 52]. However, such comparisons should be interpreted cautiously because adsorption performance can vary with pH, initial metal concentration, adsorbent dosage, particle size, ionic strength, and solution composition. Therefore, the adsorption capacities observed in this study should not be interpreted as evidence that MPs are effective Cd removal materials. Instead, the results highlight that MPs can act as environmental carriers whose polymer-dependent surface properties may influence Cd partitioning and transport.

These polymer-dependent differences likely reflect contrasts in surface chemistry and interfacial properties. FTIR spectra showed pronounced ester-related features for PLA (C=O and C–O/C–O–C), and oxygen-containing functional groups are commonly implicated as key binding functional groups for metal ions, contributing to higher adsorption affinity and capacity [53, 54]. Evidence from other aqueous adsorption systems also shows that surface chemistry, including functional groups, material components, and available binding sites, can strongly influence ion adsorption

behaviour [55]. Unlike PLA, PVC does not intrinsically contain oxygen-bearing functional groups; instead, its surface chemistry is characterised by polar C–Cl bonds. These polar bonds can increase surface polarity and promote electrostatic or dipole-related interactions with Cd, which may explain why PVC exhibits intermediate adsorption behaviour between PLA and PE [56]. By contrast, PE is dominated by non-polar $–CH_2–$ groups and lacks polar functional groups, resulting in the weakest Cd adsorption among the three polymers [33, 56].

The surface electrostatic properties support the same trend. At pH 6, zeta potentials showed a clear gradient (Table 1): PE was least negative (≈ −11 to −13 mV), PVC intermediate (≈ −22 to −24 mV), and PLA most negative (≈ −32 to −38 mV). This ordering is consistent with the adsorption trend, suggesting that a more negative surface charge favours interfacial enrichment and retention of Cd [57, 58]. The zeta-potential and Cd uptake results indicate that electrostatic attraction contributed to Cd adsorption, but it should not be interpreted as the sole controlling mechanism. The FTIR results indicate that oxygen-containing functional groups, especially the ester-related C=O and C–O/C–O–C groups in PLA, may provide binding sites for Cd through surface complexation or coordination. SEM observations further showed that PLA had a rougher and more cracked surface than PE and PVC, which may increase the accessibility of adsorption sites and promote Cd retention. Therefore, the higher Cd adsorption by PLA was likely controlled by multiple surface characteristics, including surface charge, functional groups, and surface morphology. Notably, PLA is a biodegradable polyester, and its chemistry and transformation pathways differ from conventional plastics such as PE and halogenated polymers such as PVC. Biodegradable polyesters are generally more susceptible to hydrolysis and oxidation, which can generate additional oxygenated functionalities and increase surface polarity, thereby enhancing metal-ion adsorption [59]. The markedly stronger Cd adsorption observed for PLA, therefore, likely reflects not only polymer-type differences but also broader distinctions between polyester-based biodegradable polymers and more chemically inert conventional plastics in MPs–metal interactions [46].

Effect of MP Ageing on Cd Adsorption Capacity

Ageing affected Cd adsorption in a polymer-specific manner, and its primary effect in this study was to alter the rate of Cd capture at low concentrations rather than substantially increase the ultimate adsorption capacity. In other words, the ageing effect is better interpreted as a change in surface reactivity and interfacial binding strength than as a marked increase in the total number of saturable sites. This interpretation is consistent with the fitting outcomes, in which ageing was reflected more clearly by affinity-related parameters (K_L, C_{50}, and S_0) than by Q_{max}, and it provides a mechanistic basis for the more pronounced ageing effect observed for PLA and PVC than for PE.

For PLA, which exhibited the most pronounced ageing response, the enhanced Cd uptake can be attributed to ageing-induced increases in surface polarity and the formation of additional potential binding sites. The FTIR spectra (Fig. 2) showed stronger oxygen-related features after ageing (including the carbonyl and C–O/C–O–C regions and the emergence of a broad O–H band), which are widely considered relevant to Cd binding through coordination/complexation interactions [46, 53]. Meanwhile, ageing shifted the zeta potential to more negative values (Table 1) and increased surface roughness and cracking (Fig. 1), both of which may promote interfacial enrichment of Cd and improve access to reactive sites [46, 60]. PVC showed a more modest enhancement. Given the comparatively limited evidence for new oxygenated groups from FTIR, the improved uptake of aged PVC is more plausibly attributed to changes in surface charge and morphology that increase the probability of interfacial association with Cd [21, 58]. By contrast, PE changed little under the present conditions: FTIR did not show clear formation of new oxygenated groups, suggesting that chemical oxidation introduced few additional high-affinity sites. The kinetic analysis provides further support for this polymer-specific pattern. Based on the PSO-derived initial adsorption rate ($h = k_2 \cdot qe\_cal^2$), ageing slightly increased the early-stage uptake for PE and PVC, whereas for PLA the aged material showed a higher *qe_exp* but a lower *h* than the virgin sample (Table 3). This indicates that ageing can enhance equilibrium uptake and/or binding strength without necessarily accelerating the apparent initial uptake, and the balance between these effects may differ among polymers. A cautious interpretation is that ageing may increase the availability and/or affinity of binding sites, while the apparent early-stage uptake is modulated by surface heterogeneity and/or mass-transfer constraints; however, this point would require dedicated diffusion/transport analysis to confirm.

The weak ageing effect observed for PE may also reflect the ageing protocol. Chemical ageing was carried out in 30% H_2O_2, and PE may remain near the surface because of its lower density (0.883 g/cm^3) than the solution (1.11 g/cm^3), potentially reducing effective contact with the oxidant even under shaking. Reduced contact would constrain oxidative functionalisation and surface roughening, thereby dampening any adsorption enhancement. More generally, different laboratory ageing pathways (e.g., UV photo-oxidation, thermal oxidation, and chemical oxidation) are known to generate distinct surface chemistries and adsorption behaviours [61]. H_2O_2 treatment mainly represents chemical oxidation and may introduce oxygen-containing functional groups depending on polymer reactivity and contact with the oxidant. UV ageing may additionally cause photo-oxidation, chain scission, surface cracking, and changes in crystallinity, which could modify the number and

accessibility of Cd-binding sites [49]. Natural ageing is likely to be more complex because MPs may experience combined effects of sunlight, mechanical abrasion, temperature variation, biofilm formation, and organic matter coating [62]. These processes may enhance Cd adsorption by increasing surface roughness and oxygenated functionalities, but they could also reduce apparent adsorption if biofilms or organic coatings block reactive sites or alter Cd speciation near the MP surface [62]. Therefore, the present results should be interpreted as the effect of one oxidative ageing pathway, and ageing effects may differ under UV or natural ageing conditions. Overall, ageing effects are likely controlled by polymer chemistry, ageing pathway, and exposure conditions.

Environmental Relevance and Limitations

The adsorption experiments in this study were conducted in Cd aqueous solutions prepared with ultrapure water and adjusted to pH 6.0. This controlled solution system was used to reduce the influence of background ions, dissolved organic matter, and variable ionic strength, allowing the effects of polymer type and oxidative ageing on Cd adsorption to be compared more directly. The relatively high nominal Cd concentrations were selected to generate a broad concentration range for isotherm fitting and to evaluate concentration-dependent adsorption behaviour, while lower concentrations, including 0.5, 1, and 2 mg/L, were included to capture adsorption responses at the low end of the tested range. However, natural aquatic environments and soil porewater have more complex chemical compositions, and Cd concentrations in these systems may also be lower than those used in the upper concentration range of this study. Coexisting cations and anions, dissolved organic matter, suspended particles, mineral surfaces, pH variation, and ionic strength may affect Cd speciation, MP surface charge, and the availability of adsorption sites. Therefore, the adsorption parameters obtained here should be interpreted as comparative indicators under controlled aqueous conditions rather than direct estimates of Cd adsorption in complex environmental matrices. Further studies using natural water, soil porewater, trace Cd concentrations, or soil transport systems are needed to determine whether the polymer-type and ageing-related differences observed here persist under more environmentally complex conditions.

In addition, only the 75-150 μm size fraction was tested in this study to minimise the confounding effect of particle size and allow direct comparison among polymer types and ageing states. MP size can strongly influence Cd adsorption behaviour. Smaller MPs, especially nano-sized particles, generally have larger specific surface areas, higher surface reactivity, and greater mobility [63], which may increase Cd adsorption capacity and alter Cd transport behaviour. Larger MPs may have lower adsorption capacity per unit mass because of their smaller specific surface area, although they may still influence Cd retention through surface heterogeneity, ageing, and physical interactions with surrounding media [64]. SEM-EDS was used primarily as a qualitative tool to visualise surface-associated Cd and its spatial distribution rather than to quantify adsorption. The absence of Cd signals on PVC and aged PE under the present mapping conditions (Fig. 6) may reflect the EDS detection limit and heterogeneous surface loading. Polymer-type comparisons are therefore primarily supported by quantitative solution-phase results (isotherm and kinetic parameters), while SEM–EDS provides complementary evidence of spatial heterogeneity in Cd association across polymer surfaces. Future studies could further validate surface-associated Cd by digesting the exposed MPs followed by ICP-MS or ICP-OES analysis, or using surface-sensitive techniques such as XPS to quantify Cd distribution and chemical binding states.

Finally, the role of oxygen-containing functional groups was inferred mainly from FTIR spectra, zeta potential, surface morphology, and adsorption behaviour. Although these results provide consistent evidence for stronger Cd binding by PLA, FTIR does not quantify surface elemental composition or chemical states. Quantitative surface-sensitive techniques, such as XPS, would help distinguish different oxygen-containing species and clarify their relative contribution to Cd binding.

Conclusions

This study investigated Cd adsorption on PE, PVC, and PLA MPs and evaluated the effect of oxidative ageing. Polymer type was the dominant control on Cd uptake, with a consistent ranking of PLA>PVC>PE for both virgin and aged materials. Overall, the adsorption data were better described by the Langmuir isotherm model and the pseudo-second-order kinetic model, indicating site-limited adsorption with apparent saturation behaviour and consistent time-dependent uptake patterns across polymers. Compared with PE and PVC, PLA showed higher Q_{max} and stronger affinity-related behaviour (K_L, C_{50} and S_0), consistent with its more oxygenated surface chemistry, more negative surface charge, and greater surface roughness. Ageing affected adsorption in a polymer-specific manner, primarily enhancing affinity, most clearly for PLA and to a lesser extent for PVC, while Q_{max} changed only slightly. Overall, biodegradable polyesters such as PLA may develop stronger metal-binding capacity with ageing, with implications for Cd transport in aquatic environments. This study examined how MPs of various polymer types and ageing states adsorb Cd in a controlled aqueous environment. It offers mechanistic evidence that polymer type influences MPs–Cd interactions. However, the experimental setup was deliberately simplified, using ultrapure water, fixed pH,

and minimal ionic strength, to focus solely on intrinsic polymer and ageing effects. This simplification means it does not reflect the complexity of natural environments. Future research should determine whether the polymer-type dependence observed here applies to real-world conditions and whether it impacts Cd partitioning and mobility in more complex media, such as natural water and soil, where dissolved organic matter, background electrolytes, mineral surfaces, and competing ions influence Cd speciation and transport. Soil transport experiments, such as column leaching and/or mesocosm studies, combined with realistic water chemistry and solid-phase components, could clarify the implications of polymer-specific Cd binding for Cd migration and environmental risk.

Acknowledgments

This work was supported by the Major Science and Technology Project of Guizhou Province (Qiankehe Zhongda (2025) 0041) and the High-Level Talent Training Program in Guizhou Province (GCC [2023] 045).

Conflict of Interest

The authors declare no conflict of interest.

AI Usage Disclosure Statement

While preparing this manuscript, the authors employed ChatGPT to enhance language, correct grammar, and clarify English expressions. The AI was not involved in generating data, designing experiments, performing statistical analyses, creating figures, interpreting results, or forming scientific conclusions. All AI-assisted content was thoroughly reviewed, edited, validated, and approved by the authors. The authors assume full responsibility for the manuscript's accuracy, integrity, and originality.

References

1. PRIYA A.K., JALIL A.A., DUTTA K., RAJENDRAN S., VASSEGHIAN Y., QIN J., SOTO-MOSCOSO M. Microplastics in the environment: Recent developments in characteristic, occurrence, identification and ecological risk. Chemosphere, **298**, 134161, **2022**.
2. PASTORINO P., BARCELÓ D. Microplastics and their environmental effects. Environmental Toxicology and Pharmacology, **104**, 104324, **2023**.
3. CUSWORTH S.J., DAVIES W.J., MCAINSH M.R., GREGORY A.S., STORKEY J., STEVENS C.J. Agricultural fertilisers contribute substantially to microplastic concentrations in UK soils. Communications Earth & Environment, **5** (1), 7, **2024**.
4. DENG L., LI G., PENG S., WU J., CHE Y. Microplastics in personal care products: exploring public intention of usage by extending the theory of planned behaviour. Science of the Total Environment, **848**, 157782, **2022**.
5. GHOSH S., SINHA J.K., GHOSH S., VASHISTH K., HAN S., BHASKAR R. Microplastics as an emerging threat to the global environment and human health. Sustainability, **15** (14), 10821, **2023**.
6. CHAIRUNNISA N.K., ADAM M.A., KRISTIANTO S., CANDRI D.A., TALBIA H.S., APRILIA M., MUTIA T., MASRUROH H., ISWARA A.P., PRAYOGO W. Linking the tourism activity to the occurrence and distribution of microplastics. Civil Engineering Journal, **11** (7), 2811, **2025**.
7. CAI Z., LI M., ZHU Z., WANG X., HUANG Y., LI T., GONG H., YAN M. Biological degradation of plastics and microplastics: a recent perspective on associated mechanisms and influencing factors. Microorganisms, **11** (7), 1661, **2023**.
8. DISSANAYAKE P.D., KIM S., SARKAR B., OLESZCZUK P., SANG M.K., HAQUE M.N., AHN J.H., BANK M.S., OK Y.S. Effects of microplastics on the terrestrial environment: A critical review. Environmental Research, **209**, 112734, **2022**.
9. MEJJAD N., SAFHI A.E.M., LAISSAOUI A. Insightful analytical review of potential impacts of microplastic pollution on coastal and marine ecosystem services. Journal of Hazardous Materials Advances, **17**, 100578, **2025**.
10. IDBELLA M., DJEBAILI R., IDBELLA A., ABELOUAH M.R., IACOMINO G., PELLEGRINI M., BONANOMI G. Impact of microplastics on soil microbiota and phosphorus dynamics-a review. Emerging Contaminants, **12** (2), 100663, **2026**.
11. LI Q., BOGUSH A., VAN DE WIEL M., WU P., HOLTZMAN R. Microplastics transport in soils: A critical review. Earth-Science Review, **264**, 105108, **2025**.
12. ULLAH F., WANG P.Y., SAQIB S., ZHAO L., ASHRAF M., KHAN A., KHAN W., KHAN A., CHEN Y., XIONG Y.C. Toxicological complexity of microplastics in terrestrial ecosystems. Iscience, **28** (2), 111879, **2025**.
13. QU F., ZHENG W. Cadmium exposure: mechanisms and pathways of toxicity and implications for human health. Toxics, **12** (6), 388, **2024**.
14. JAISHANKAR M., TSETEN T., ANBALAGAN N., MATHEW B.B., BEEREGOWDA K.N. Toxicity, mechanism and health effects of some heavy metals. Interdisciplinary Toxicology, **7** (2), 60, **2014**.
15. YUAN Z., LUO T., LIU X., HUA H., ZHUANG Y., ZHANG X., ZHANG L., ZHANG Y., XU W., REN J. Tracing anthropogenic cadmium emissions: From sources to pollution. Science of the Total Environment, **676**, 87, **2019**.
16. KHAN M.A., KHAN S., KHAN A., ALAM M. Soil contamination with cadmium, consequences and remediation using organic amendments. Science of the Total Environment, **601**, 1591, **2017**.
17. SUN H., SHAO C., JIN Q., LI M., ZHANG Z., LIANG H., LEI H., QIAN J., ZHANG Y. Effects of cadmium contamination on bacterial and fungal communities in Panax ginseng-growing soil. BMC Microbiology, **22** (1), 77, **2022**.
18. MALIK I.S., KHAN Z.I., AHMAD K., NADEEM M., AKHTAR S., ASHFAQ A., ULLAH S. Food chain risk assessment of cadmium accumulation and the relationships

among diversely irrigated pasture-reared ruminants. Scientific Reports, **15** (1), 34868, **2025**.
19. ZHANG Z., LI Y., QIU T., DUAN C., CHEN L., ZHAO S., ZHANG X., FANG L. Microplastics addition reduced the toxicity and uptake of cadmium to Brassica chinensis L. Science of the Total Environment, **852**,158353, **2022**.
20. HUANG F., HU J., CHEN L., WANG Z., SUN S., ZHANG W., JIANG H., LUO Y., WANG L., ZENG Y., FANG L. Microplastics may increase the environmental risks of Cd via promoting Cd uptake by plants: A meta-analysis. Journal of Hazardous Materials, **448**, 130887, **2023**.
21. LI F., YANG X., ZHANG Z., JIANG Y., GONG Y. Behaviour, ecological impacts of microplastics and cadmium on soil systems: A systematic review. Environmental Technology & Innovation, **35**, 103637, **2024**.
22. XIONG X., WANG J., LIU J., XIAO T. Microplastics and potentially toxic elements: A review of interactions, fate and bioavailability in the environment. Environmental Pollution, **340**, 122754, **2024**.
23. KUMAR R., IVY N., BHATTACHARYA S., DEY A., SHARMA P. Coupled effects of microplastics and heavy metals on plants: Uptake, bioaccumulation, and environmental health perspectives. Science of the Total Environment, **836**, 155619, **2022**.
24. KHALID N., AQEEL M., NOMAN A., KHAN S.M., AKHTER N. Interactions and effects of microplastics with heavy metals in aquatic and terrestrial environments. Environmental Pollution, **290**, 118104, **2021**.
25. ERDEM H., GENCE C.Ç., ÖZTÜRK M., BUHAN E., KHOLIKULOV S.T., KAYA Y. Microplastics in Soil Increase Cadmium Toxicity: Implications for Plant Growth and Nutrient Imbalance. Water Air and Soil Pollution, **236** (9),1, **2025**.
26. CAO Y., MA X., CHEN N., CHEN T., ZHAO M., LI H., SONG Y., ZHOU J., YANG J. Polypropylene microplastics affect the distribution and bioavailability of cadmium by changing soil components during soil aging. Journal of Hazardous Materials, **443**, 130079, **2023**.
27. HUANG F., CHEN L., YANG X., JEYAKUMAR P., WANG Z., SUN S., QIU T., ZENG Y., CHEN J., HUANG M., WANG H. Unveiling the impacts of microplastics on cadmium transfer in the soil-plant-human system: A review. Journal of Hazardous Materials, **477**, 135221, **2024**.
28. LIU G., GU X., WU J., LI H., SU L., CHEN M., CHEN S., LIU Y. The interaction effects of biodegradable microplastics and Cd on Folsomia candida soil collembolan. Environmental Science and Pollution Research, **30** (19), 57041, **2023**.
29. LI W., ZU B., YANG Q., HUANG Y., LI J. Adsorption of lead and cadmium by microplastics and their desorption behavior as vectors in the gastrointestinal environment. Journal of Environmental Chemical Engineering, **10** (3), 107379, **2022**.
30. GAO F., LI J., SUN C., ZHANG L., JIANG F., CAO W., ZHENG L. Study on the capability and characteristics of heavy metals enriched on microplastics in marine environment. Marine Pollution Bulletin, **144**, 61, **2019**.
31. LUO H., TU C., HE D., ZHANG A., SUN J., LI J., XU J., PAN X. Interactions between microplastics and contaminants: A review focusing on the effect of aging process. Science of the Total Environment, **899**, 165615, **2023**.
32. WANG F., YANG W., CHENG P., ZHANG S., ZHANG S., JIAO W., SUN Y. Adsorption characteristics of cadmium onto microplastics from aqueous solutions. Chemosphere, **235**, 1073, **2019**.
33. WANG S., WANG X., WANG X., QIN Z., HU J., DING S., FENG K. Study on the Adsorption Behavior of Cadmium by the MPs and Its Environmental Factors. Polish Journal of Environmental Studies, **32** (5), 4313, **2023**.
34. HUANG W., DENG J., LIANG J., XIA X. Comparison of lead adsorption on the aged conventional microplastics, biodegradable microplastics and environmentally-relevant tire wear particles. Chemical Engineering Journal, **460**, 141838, **2023**.
35. LANG M., YU X., LIU J., XIA T., WANG Q., HAO Y. Fenton aging significantly affects the heavy metal adsorption capacity of polystyrene microplastics. Science of the Total Environment, **722**, 137762, **2020**.
36. ZHANG D., XING Y., WANG X., LI W., GUO Y., TANG Y., ZHANG H., CHEN J., JIANG B. The effect of polyvinyl chloride microplastics on soil properties, greenhouse gas emission, and element cycling-related genes: Roles of soil bacterial communities and correlation analysis. Journal of Hazardous Materials, **480**, 136248, **2024**.
37. MASCIARELLI E., CASORRI L., DI LUIGI M., BENI C., VALENTINI M., COSTANTINI E., AIELLI L., REALE M. Microplastics in agricultural crops and their possible impact on farmers' health: A review. International Journal of Environmental Research and Public Health, **22** (1), 45, **2024**.
38. LIU R., LIANG J., YANG Y., JIANG H., TIAN X. Effect of polylactic acid microplastics on soil properties, soil microbials and plant growth. Chemosphere, **329**, 138504, **2023**.
39. HIDALGO-RUZ V., GUTOW L., THOMPSON R.C., THIEL M. Microplastics in the marine environment: A review of the methods used for identification and quantification. Environmental Science & Technology, **46** (6), 3060, **2012**.
40. ZHAO S., KVALE K.F., ZHU L., ZETTLER E.R., EGGER M., MINCER T.J., AMARAL-ZETTLER L.A., LEBRETON L., NIEMANN H., NAKAJIMA R., THIEL M., BOS R.P., GALGANI L., STUBBINS A. The distribution of subsurface microplastics in the ocean. Nature, **641** (8061), 51, **2025**.
41. BHAGAT K., BARRIOS A.C., RAJWADE K., KUMAR A., OSWALD J., APUL O., PERREAULT F. Aging of microplastics increases their adsorption affinity towards organic contaminants. Chemosphere, **298**, 134238, **2022**.
42. DONG S., YAN X., YUE Y., LI W., LUO W., WANG Y., SUN J., LI Y., LIU M., FAN M. H_2O_2 concentration influenced the photoaging mechanism and kinetics of polystyrene microplastic under UV irradiation: Direct and indirect photolysis. Journal of Cleaner Production, **380**, 135046, **2022**.
43. KHAYYUN T.S., MSEER A.H. Comparison of the experimental results with the Langmuir and Freundlich models for copper removal on limestone adsorbent. Applied Water Science, **9** (8), 170, **2019**.
44. DENG S., LIU Y., GUO C., ZHOU X., LU Q., FAN Z., GAO Z., XIANG Q., JIN Z., CHEN X. Polyvinyl chloride microplastics reduce Cd (II) adsorption and enhance desorption with soil-dependent mechanisms. Environmental Technology & Innovation, **34**, 103607, **2024**.
45. BAUTISTA QUISPE J.I., CAMPOS L.C., MAŠEK O., BOGUSH A. Removal of anionic surfactant from aqueous solutions by adsorption onto biochars: characterisation, kinetics, and mechanism. Environmental Technology, **45** (26), 5723, **2024**.

46. XIAO X., HODSON M.E., SALLACH J.B. Biodegradable microplastics adsorb more Cd than conventional microplastic and biofilms enhance their adsorption. Chemosphere, **371**, 144062, **2025**.
47. BI S., LIU S., LIU E., XIONG J., XU Y., WU R., LIU X., XU J. Adsorption behavior and mechanism of heavy metals onto microplastics: A meta-analysis assisted by machine learning. Environmental Pollution, **360**, 124634, **2024**.
48. SHIMIZU S., MATUBAYASI N. Understanding sorption mechanisms directly from isotherms. Langmuir, **39** (17), 6113, **2023**.
49. HS H., S TANTRI P., G HIREMATH P., PARUN A., MUDHULU S., H PATIL J., KUSANUR R. Optimised fluoride adsorption from water using functionalised rice straw: a response surface methodology approach. International Journal of Sustainable Engineering, **19** (1), 2619282, **2026**.
50. AL-GHOUTI M.A., DA'ANA D.A. Guidelines for the use and interpretation of adsorption isotherm models: A review. Journal of Hazardous Materials, **393**, 122383, **2020**.
51. YUAN S., HONG M., LI H., YE Z., GONG H., ZHANG J., HUANG Q., TAN Z. Contributions and mechanisms of components in modified biochar to adsorb cadmium in aqueous solution. Science of the Total Environment, **733**, 139320, **2020**.
52. SUN Q., KAMARUDDIN M., HUANG K., CAO Y., YUSOFF M., CHENG Y. Study on preparation of nano humic acid and adsorption effect of heavy metals in soil. Emerging Science Journal, **9** (5), 2350, **2025**.
53. MAO R., LANG M., YU X., WU R., YANG X., GUO X. Aging mechanism of microplastics with UV irradiation and its effects on the adsorption of heavy metals. Journal of Hazardous Materials, **393**, 122515, **2020**.
54. JIANG L., CHEN Y., WANG Y., LV J., DAI P., ZHANG J., HUANG Y., LV W. Contributions of various Cd (II) adsorption mechanisms by phragmites australis-activated carbon modified with mannitol. ACS Omega, **7** (12), 10502, **2022**.
55. LÓPEZ-BERMÚDEZ N.L., RODRÍGUEZ-TORRES A.C., OTÁLVARO-ÁLVAREZ Á.M., PEÑA-GUZMÁN C.A. Phosphate adsorption from aqueous solutions using eggshell and Sacha Inchi (Plukenetia volubilis) mixture. Civil Engineering Journal, **11** (7), 2918, **2025**.
56. LIU S., SHI J., WANG J., DAI Y., LI H., LI J., LIU X., CHEN X., WANG Z., ZHANG P. Interactions between microplastics and heavy metals in aquatic environments: a review. Frontiers in Microbiology, **12**, 652520, **2021**.
57. GUI X., REN Z., XU X., CHEN X., CHEN M., WEI Y., ZHAO L., QIU H., GAO B., CAO X. Dispersion and transport of microplastics in three water-saturated coastal soils. Journal of Hazardous Materials, **424**, 127614, **2022**.
58. SHAHZAD K., HASAN A., NAQVI S.K.H., PARVEEN S., HUSSAIN A., KO K.C., PARK S.H. Recent advances and factors affecting the adsorption of nano/microplastics by magnetic biochar. Chemosphere, **370**, 143936, **2025**.
59. FAYYAZBAKHSH A., HAJINAJAF N., BAKHTIARI H., FEUCHTER M., IMPROTA I., SALEHI E., SHAHSAVAR S.K., JULINOVA M., GHASEMI A., GHASEMI B., AFSHARNIA R. Eco-friendly additives for biodegradable polyesters: Recent progress in performance optimization and environmental impact reduction. Sustainable Materials and Technologies, **44**, e01395, **2025**.
60. WANG M., JIANG X., WEI Z., WANG L., SONG J., CEN P. Enhanced cadmium adsorption dynamics in water and soil by polystyrene microplastics and biochar. Nanomaterials, **14** (13), 1067, **2024**.
61. WANG L., ZHANG J., HUANG W., HE Y. Laboratory simulated aging methods, mechanisms and characteristic changes of microplastics: A review. Chemosphere, **315**, 137744, **2023**.
62. BINDA G., KALČÍKOVÁ G., ALLAN I.J., HURLEY R., RØDLAND E., SPANU D., NIZZETTO L. Microplastic aging processes: Environmental relevance and analytical implications. TrAC Trends in Analytical Chemistry, **172**, 117566, **2024**.
63. TALLEC K., BLARD O., GONZÁLEZ-FERNáNDEZ C., BROTONS G., BERCHEL M., SOUDANT P., HUVET A., PAUL-PONT I. Surface functionalization determines behavior of nanoplastic solutions in model aquatic environments. Chemosphere, **225**, 639, **2019**.
64. TENEA A.-G., DINU C., RUS P.A., IONESCU I.A., GHEORGHE S., IANCU V.I., VASILE G.G., PASCU L.F., CHIRIAC F.L. Exploring adsorption dynamics of heavy metals onto varied commercial microplastic substrates: Isothermal models and kinetics analysis. Heliyon, **10** (15), **2024**.